

Testing the nature of Gauss-Bonnet gravity by four-dimensional rotating black hole shadow

Shao-Wen Wei ^{*} and Yu-Xiao Liu [†]

*Institute of Theoretical Physics & Research Center of Gravitation,
Lanzhou University, Lanzhou 730000, People's Republic of China,
and Joint Research Center for Physics, Lanzhou University and
Qinghai Normal University, Lanzhou 730000 and Xining 810000, China*

The recent discovery of the novel four-dimensional static and spherically symmetric Gauss-Bonnet black hole provides a promising bed to test Gauss-Bonnet gravity by using astronomical observations [Phys. Rev. Lett. 124, 081301 (2020)]. In this paper, we first obtain the rotating Gauss-Bonnet black hole solution by using the Newman-Janis algorithm, and then study the shadow cast by the nonrotating and rotating Gauss-Bonnet black holes. The result indicates that positive Gauss-Bonnet coupling parameter shrinks the shadow, while negative one enlarges it. Meanwhile, both the distortion and ratio of two diameters of the shadow are found to increase with the coupling parameter for certain spin. Comparing with the Kerr black hole, the shadow gets more distorted for positive coupling parameter, and less distorted for negative one. Furthermore, we calculate the angular diameter of the shadow by making use of the observation of M87*. The result indicates that negative dimensionless Gauss-Bonnet coupling parameter in $(-4.5, 0)$ is more favored. Therefore, our result gives a first constraint to Gauss-Bonnet gravity. We believe further study on the four-dimensional rotating black hole will shed new light on Gauss-Bonnet gravity.

PACS numbers: 04.50.Kd, 04.25.-g, 04.70.-s

I. INTRODUCTION

Nearly one year ago, Event Horizon Telescope (EHT) Collaboration released the first image of the supermassive black hole located at the center of M87 galaxy [1–6]. This fruitful outcome shows a fine structure near a black hole horizon and opens up a new window to test the strong gravity regime. The result indicates that the black hole shadow has a diameter $42 \pm 3 \mu\text{as}$. Modeled M87* with a Kerr geometry, the observations were found to be well consistent with the prediction of general relativity. However, there still exists a living space for some modified gravities due to the finite resolution. With future observations, like the Next Generation Very Large Array [7], the Thirty Meter Telescope [8], and the BlackHoleCam [9], it will offer us a good opportunity to peek into the regime of strong gravity, and to distinguish different modified gravities. Meanwhile, more knowledge and information on modified gravities and quantum gravity will be greatly revealed.

EHT observation restimulates the study of the black hole shadow. As we know, when photons are emitted from its source, then fly past a black hole, they will have three results—absorbed by the black hole, reflected by the black hole and then escaping to infinity, or surrounding the black hole one loop by one loop. These photons escaped from the black hole will illuminate the sky of an observer. However, these photons absorbed by the black hole will leave a dark zone for the observer. This dark zone is actually the black hole shadow.

As early as 1966, Synge studied the observed angular radius of a Schwarzschild black hole [10]. Later, a formula describing the shadow size was given by Luminet [11]. Now it is generally known that the shadow shape of a spherically symmetric black hole is round. While it will be elongated, for a rotating black hole, in the direction of the rotating axis due to spacetime dragging effect [12, 13]. The size and distortion of the shadow have a close relation with the spacetime geometry. Thus by constructing different observables, a number of papers concern how do these observables depend on the parameters of the black hole spacetime [14–61]. There are other related works [62–70] that aim to constrain

^{*} weishw@lzu.edu.cn

[†] liuyx@lzu.edu.cn, corresponding author.

the parameters of the black holes or other compact objects from astronomical observations of M87*. Moreover, it is also expected to cast deep insight into modified gravities.

In the past few decades, different modified gravity theories were proposed with the attempt to solve the fundamental questions, such as the quantum gravity and singularity problem. Among them, Gauss-Bonnet (GB) gravity including higher curvature corrections is one of the most promising approaches. It is well known for a long time that there exist different static and spherically symmetric black hole solutions from general relativity in d -dimensional spacetime with $d > 4$. While no different black hole solution exists in four dimensions due to that the GB term is a total derivative, and thus it has no contribution to the gravitational dynamics. Since the dimension of the observed spacetime is four, it is extremely hard to test the nature of GB gravity through astronomical observations.

In Refs. [71, 72], the authors considered the GB gravity in four dimensions by rescaling the GB coupling parameter $\alpha \rightarrow \frac{\alpha}{d-4}$. Very recently, Glavan and Lin [73] reconsidered this issue and proposed a general covariant modified gravity in four dimensions, in which only the massless graviton propagates. It can also bypass the Lovelock's theorem and avoid Ostrogradsky instability. Taking the dimension number $d \rightarrow 4$, the GB term shows a nontrivial contribution to the gravitational dynamics. And then a nontrivial and novel four-dimensional static and spherically symmetric black hole solution was discovered. Such black hole, in particular, offers us a promising bed to test the nature of GB gravity. Subsequently, the quasinormal modes of scalar, electromagnetic and gravitational perturbations were calculated in [74], where the results show that varying with the GB coupling parameter, the damping rate is more sensitive characteristic than the real part. Dynamical eikonal instability occurs for larger GB coupling parameter. The shadow cast by the spherically symmetric black hole was examined in Refs. [74, 75]. The shadow size exhibits a close relation with the coupling parameter. In addition, all the radii of the innermost stable circular orbit, black hole horizon, and the photon sphere are decreasing functions of the GB coupling parameter [75]. This black hole solution was generalized to the charged case [76]. The cosmological and black hole solutions arising from the gravity was also discussed in Ref. [77].

Although this novel gravity admits a nontrivial contribution in four dimensions, there are works concerning about whether this gravity makes sense in general. Different multiple pathologies were pointed out in Refs. [78–86]. For example in Ref. [80], the authors showed that such gravity does not admit a description in terms of a covariantly-conserved rank-2 tensor in four dimensions. Other references argued that the dimensional regularization procedure is ill-defined in a general spacetime. However, some regularized 4D EGB theories were presented in Refs. [87–89]. The regularization procedures include introducing an extra GB term constructed by a conformal metric [88, 89] and compactification of the D -dimensional EGB theory [87]. The resulting gravity has an extra scalar degree of freedom which helps us to obtain the field equations in a 4D version. Generally, it is believed that the regularization can be applied to the maximally symmetric or spherical symmetric space in 4D spacetimes, while may be problematic for the case of the axially symmetric case [89]. This approach suggests that the GB gravity belongs to the family of Horndeski gravity. Following Ref. [82], the treatment was also found to be applicable in a spacetime with low symmetry, for example the cylindrically symmetric spacetime [86]. However, it is worth to check this also works for the axially symmetric spacetime. Nevertheless, it is still worth to investigate the novel properties of the black hole solution in this gravity.

It is generally believed that almost all the astronomical black holes have spin. So it is worth to study the particular properties for the rotating black hole, which will provide us opportunities to test the nature of GB gravity by using astronomical observations, especially the observations of M87* by the EHT Collaboration. In this paper, we mainly focus on studying the shadow cast by the GB black hole, and constraining the GB coupling parameter. So we first generalize the black hole to a rotating one by using the Newman-Janis (NJ) algorithm [90]. Although it was found in Ref. [91] that the NJ trick is not generally applicable in higher curvature theories, the solution might describe a black hole with matter fields such as the fluids [92]. Therefore, it is worth to study the rotating black hole in this GB gravity. Then, by modeling M87* with this rotating GB black hole, we constraint the GB coupling parameter via the observations of EHT Collaboration. The result reveals that negative GB coupling parameter is more favored. Another study on the shadow in Einstein-dilaton-Gauss-Bonnet black holes can be found in Ref. [93].

The paper is organized as follows. In Sec. II, we first show the nonrotating GB black hole solution, and then extend it to its rotating counterpart by the NJ algorithm. Different regions of the spacetime in the parameter space are also displayed. Null geodesics and circular photon orbit are given in Sec. III. In Sec. IV, the shadow shapes are exhibited. Basing on them, we construct several observables and obtain their behaviors with the spin and GB coupling parameter, which provides us the preliminary nature on the four-dimensional GB black hole. Comparing with the Kerr black hole, we observe that positive coupling shrinks the shadow, while negative coupling enlarges it. Then, after obtaining these results, we constraint the GB coupling parameter by calculating the angular diameter of the shadow via the observation of M87* in Sec. V. Finally, the conclusions and discussions are presented in Sec. VI.

II. FOUR-DIMENSIONAL GAUSS-BONNET BLACK HOLE

In this section, we will focus on the properties of the four-dimensional nonrotating and rotating black holes.

A. Non-rotating black hole

In GB gravity, it is well known that there are the static and spherically symmetric black hole solutions in a spacetime with $d \geq 5$, for examples see Refs. [94–98]. However, in four-dimensional spacetime, the GB term is a total derivative, and thus it has no contribution to the gravitational dynamics. Until recently, a four-dimensional nontrivial black hole was discovered by Glavan and Lin [73]. They first rescaled the GB coupling parameter $\alpha \rightarrow \alpha/(d-4)$, then took the limit $d \rightarrow 4$, and finally found a static and spherically symmetric black hole solution [73]

$$ds^2 = f(r)dt^2 - \frac{dr^2}{f(r)} - r^2(d\theta^2 + \sin^2\theta d\phi^2), \quad (1)$$

$$f(r) = 1 + \frac{r^2}{2\alpha} \left(1 - \sqrt{1 + \frac{8\alpha M}{r^3}} \right). \quad (2)$$

This black hole solution exactly coincides with that obtained in a gravity with conformal anomaly [99, 100]. Here M is the black hole mass. This solution can be obtained by solving the following action

$$S = \int \sqrt{-g}d^4x (R + \alpha L_{GB}), \quad (3)$$

$$L_{GB} = R_{\mu\nu\rho\sigma}R^{\mu\nu\rho\sigma} - 4R_{\mu\nu}R^{\mu\nu} + R^2, \quad (4)$$

where we have taken $16\pi G = 1$. This solution can bypass the Lovelock's theorem and avoid Ostrogradsky instability. When $r \rightarrow 0$ and $r \rightarrow \infty$, we have

$$f(r \rightarrow 0) = 1 - \sqrt{\frac{2M}{\alpha}}r^{\frac{1}{2}} + \frac{1}{2\alpha}r^2 + \mathcal{O}\left(r^{\frac{7}{2}}\right), \quad (5)$$

$$f(r \rightarrow \infty) = 1 - \frac{2M}{r} + \frac{4\alpha M^2}{r^4} + \mathcal{O}\left(\frac{1}{r^7}\right). \quad (6)$$

So, this metric is asymptotic flat. As we know, GB gravity arises from low energy limit from heterotic string theory. The GB coupling parameter α has dimensions of the square of length and plays the role of the inverse string tension. The black hole horizons can be obtained by solving $f(r) = 0$, which gives

$$r_{\pm} = M \pm \sqrt{M^2 - \alpha}. \quad (7)$$

For positive α , we have two horizons for $\alpha/M^2 < 1$, one degenerate horizon (corresponding to an extremal black hole) for $\alpha/M^2 = 1$, while no horizon for $\alpha/M^2 > 1$. Although α acts as the inverse string tension and should be positive, the solution (2) allows the existence of a negative α . This might extend the conventional GB gravity. So it is interesting to examine the properties of this extended GB gravity with a negative α . We expect some interesting properties could be revealed. For negative α , it was argued in Ref. [73] that no real solution exists at short radial distances when $r^3 < -8\alpha M$. However it was noted that in the range $-8 \leq \alpha/M^2 < 0$, the singular short radial distances are always hidden inside the outer horizon r_+ [75], which therefore provides a well behaved external solution. Therefore, we consider the black hole solution in the region $-8 \leq \alpha/M^2 < 1$ in this paper.

B. Rotating black hole

In this subsection, we would like to adopt the NJ algorithm [90] to generate the rotating GB black hole solution from (1) by following the approach [92].

First, we introduce the Eddington-Finkelstein coordinates (u, r, θ, ϕ) with

$$du = dt - \frac{dr}{f(r)}. \quad (8)$$

Then the metric of the nonrotating GB black hole becomes

$$ds^2 = f(r)du^2 + 2dudr - r^2d\theta^2 - r^2\sin^2\theta d\phi^2. \quad (9)$$

Further, the metric can be expressed as

$$g^{ab} = l^a m^b + l^b n^a - m^a \bar{m}^b - m^b \bar{m}^a, \quad (10)$$

with the null tetrads given by [92]

$$l^a = \delta_r^a, \quad (11)$$

$$n^a = \delta_\mu^a - \frac{f(r)}{2}\delta_r^a, \quad (12)$$

$$m^a = \frac{1}{\sqrt{2}r} \left(\delta_\theta^a + \frac{i}{\sin\theta} \delta_\phi^a \right). \quad (13)$$

It is easy to find that these null tetrads have the following relations:

$$l^a l_a = n^a n_a = m^a m_a = \bar{m}^a \bar{m}_a = 0, \quad (14)$$

$$l^a m_a = l^a \bar{m}_a = n^a m_a = n^a \bar{m}_a = 0, \quad (15)$$

$$l^a n_a = -m^a \bar{m}_a = 1. \quad (16)$$

Now, we perform the complex coordinate transformations in (u, r) -plane following the NJ algorithm

$$\begin{aligned} u' &\rightarrow u - ia \cos\theta, \\ r' &\rightarrow r + ia \cos\theta, \end{aligned} \quad (17)$$

with a a spin parameter of the black hole.

Next step is complexifying the radial coordinate r in the NJ algorithm. However it is not necessary. As shown by [92], this complexifying process can be dropped by considering that δ_ν^μ transforms as a vector under (17). At the same time the metric functions of (9) transform to new undetermined ones

$$f(r) \rightarrow F(r, a, \theta), \quad (18)$$

$$r^2 \rightarrow H(r, a, \theta). \quad (19)$$

After this transformation, the null tetrads become

$$l^a = \delta_r^a, \quad (20)$$

$$n^a = \delta_\mu^a - \frac{F}{2}\delta_r^a, \quad (21)$$

$$m^a = \frac{1}{\sqrt{2}H} \left((\delta_\mu^a - \delta_r^a)ia \sin\theta + \delta_\theta^a + \frac{i}{\sin\theta} \delta_\phi^a \right). \quad (22)$$

Making use of the new null tetrads, the rotating metric in the Eddington-Finkelstein coordinates is given by

$$\begin{aligned} ds^2 = & F du^2 + 2dudr + 2a \sin^2\theta (1 - F) dud\phi - 2a \sin^2\theta dr d\phi \\ & - H d\theta^2 - \sin^2\theta (H + a^2 \sin^2\theta (1 - F)) d\phi^2. \end{aligned} \quad (23)$$

Bringing this coordinates back to the Boyer-Lindquist ones, we can obtain the rotating GB black hole. In order to achieve it, we introduce a global coordinate transformation

$$du = dt + \lambda(r)dr, \quad (24)$$

$$d\phi = d\phi' + \chi(r)dr, \quad (25)$$

with [92]

$$\lambda(r) = -\frac{a^2 + r^2}{a^2 + r^2 f(r)}, \quad (26)$$

$$\chi(r) = -\frac{a}{a^2 + r^2 f(r)}. \quad (27)$$

At last, we choose

$$F = \frac{(r^2 f(r) + a^2 \cos^2 \theta)}{H}, \quad (28)$$

$$H = r^2 + a^2 \cos^2 \theta. \quad (29)$$

Then the rotating black hole metric reads

$$ds^2 = -\frac{\Delta}{\rho^2} (dt - a \sin^2 \theta d\phi)^2 + \frac{\rho^2}{\Delta} dr^2 + \rho^2 d\theta^2 + \frac{\sin^2 \theta}{\rho^2} (adt - (r^2 + a^2)d\phi)^2. \quad (30)$$

Note that, we have changed the sign of the metric according to the convention. For the four-dimensional rotating GB black hole, the metric functions are

$$\rho^2 = r^2 + a^2 \cos^2 \theta, \quad (31)$$

$$\Delta = r^2 + a^2 + \frac{r^4}{2\alpha} \left(1 - \sqrt{1 + \frac{8\alpha M}{r^3}} \right). \quad (32)$$

It is worth to point out that a couple of days later after we submitted this paper to arXiv, there appears another paper concerning the same rotating black hole case and its shadow [101]. We have set $16\pi G=1$ in the action, so both the two black hole solutions are the same. Here we would like to give a comment on the above black hole solution. Since we cannot write out the field equations, it is extremely hard to directly check the solution (30). On the other hand, one can check the trace of the field equations, $R = -\frac{\alpha}{2} L_{GB}$, where the rescaling $\alpha \rightarrow \alpha/(d-4)$ has been done. It is easy to find that the trace equation holds for $\theta = \pi/2$, which is because that the spacetime has a higher symmetry on the equatorial plane. While the case behaves differently when it deviates this plane. After the NJ algorithm, we argue that some matter fields such as fluids or scalar fields are introduced in the GB action [92]. So the solution obtained here is not the GB vacuum solution. On the other hand, as we know, in GR, the Kerr solution can be obtained from a Schwarzschild one by using the NJ algorithm, and both black holes are the vacuum solutions. However, when applying the NJ algorithm to the four-dimensional GB black hole, the rotating one is not a vacuum solution anymore. This as one wishes may be related to the pathological behaviour of the four-dimensional novel GB gravity, where only highly symmetric spacetimes make sense. For spacetimes with low symmetry, some matter fields must be included. Furthermore, considering the gravitational field equations, one can calculate the energy-momentum tensor. However, for this four-dimensional GB gravity, one could not do this since there is no explicit field equations. But this could be resolved according to Refs. [87–89], where some regularized 4D EGB theories were constructed and the gravitational field equations were given. When the spin $a = 0$, this metric will reduce to the static and spherically symmetric one (1). On the other hand, at the small α limit, we have

$$\Delta(\alpha \rightarrow 0) = \Delta_{Kerr} + \frac{4M^2}{r^2} \alpha + \mathcal{O}(\alpha^2), \quad (33)$$

where $\Delta_{Kerr} = r^2 - 2Mr + a^2$ for the Kerr black hole. It is clear that the GB coupling parameter α modifies the Kerr solution.

The horizons of the black hole can be obtained by solving $\Delta = 0$. For positive $0 \leq \alpha/M^2 \leq 1$, it is similar with the Kerr case. There can be two horizons, one horizon, and no horizon. There exists a maximal value of spin a for certain α , beyond which only the naked singularity is presented. While for negative α , only one positive real root of $\Delta = 0$ is found, which indicates that there only exists one black hole horizon. Also, similar to the nonrotating black hole, the solution only exists for

$$r \geq r_0 = 2(-\alpha M)^{\frac{1}{3}}. \quad (34)$$

In order to guarantee the existence of the horizon and $r_+ \geq r_0$, one should have $\Delta(r_0) \leq 0$, which requires that the black hole spin satisfies the following relation

$$a^2/M^2 \leq 4(-\alpha/M^2)^{\frac{1}{3}} \left(2 - (-\alpha/M^2)^{\frac{1}{3}} \right). \quad (35)$$

At $\alpha = -M^2$, the spin approaches its maximum $2M$. In Fig. 1, we show the different regions of the spacetime in a/M - α/M^2 plane. In regions I and II, they are black holes with two and one horizon, respectively. Region III is for the naked singularity. Differently, in region IV, the spacetime has no horizon and has no real solution at the short radial distances. Therefore, we only consider the black hole regions I and II. Although the rotating black hole is not a vacuum solution in this GB gravity. It still worths to examine its gravitational effects. And this might show some interesting properties of this four-dimensional GB gravity.

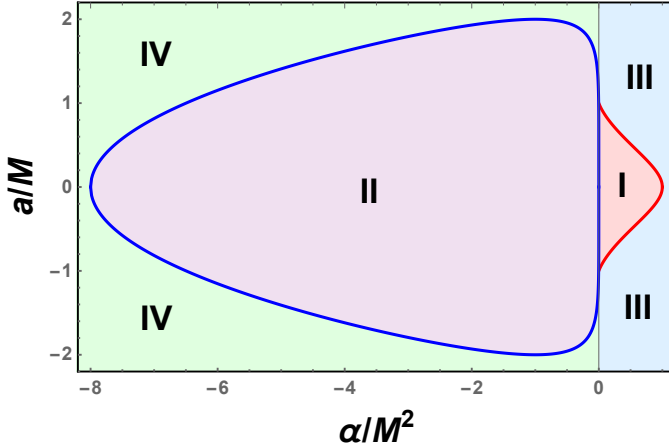


FIG. 1: Regions I and II are black holes with two and one horizon, respectively. Region III is for the naked singularity. In region IV, the spacetime does not have horizon and real solution at the short radial distances.

III. GEODESICS AND CIRCULAR PHOTON ORBITS

In this section, we would like to investigate the geodesics in the background of (30). We will study the circular photon orbits of the black hole, which is a key quantity on examining the shadows cast by the four-dimensional GB black hole.

The geodesics of a particle moving in this background can be obtained by solving the geodesic equation. Alternately, one can adopt the Hamilton-Jacobi approach. The Hamilton-Jacobi equation describing the particle is

$$\frac{\partial S}{\partial \lambda} = -\frac{1}{2}g^{\mu\nu}\frac{\partial S}{\partial x^\mu}\frac{\partial S}{\partial x^\nu}, \quad (36)$$

where λ is the the affine parameter. For this black hole background, there are two Killing fields ∂_t and ∂_ϕ , which give us two constants, the particle energy E and orbital angular momentum l along each geodesics

$$-E = g_{t\mu}\dot{x}^\mu, \quad (37)$$

$$l = g_{\phi\mu}\dot{x}^\mu. \quad (38)$$

Then the Jacobi action can be separated as

$$S = \frac{1}{2}\mu^2\lambda - Et + l\phi + S_r(r) + S_\theta(\theta), \quad (39)$$

where μ^2 is the rest mass of the particle. The functions $S_r(r)$ and $S_\theta(\theta)$, respectively, depends only on r and θ . Substituting the Jacobi action (39) into the Hamilton-Jacobi equation (36), one obtains

$$S_r(r) = \int^r \frac{\sqrt{\mathcal{R}(r)}}{\Delta(r)} dr, \quad (40)$$

$$S_\theta(\theta) = \int^\theta \sqrt{\Theta(\theta)} d\theta, \quad (41)$$

with

$$\mathcal{R} = \left[(r^2 + a^2)E - al \right]^2 - \Delta \left[\mu^2 r^2 + \mathcal{K} + (l - aE)^2 \right], \quad (42)$$

$$\Theta = \mathcal{K} + \cos^2 \theta (a^2(E^2 - \mu^2) - l^2 \sin^{-2} \theta), \quad (43)$$

where the Carter parameter \mathcal{K} related to the Killing-Yano tensor field is another constant of the geodesics. Further combining $g_{\mu\nu}\dot{x}^\mu\dot{x}^\nu = -\mu^2$, we can obtain the following equation of motion for the particle in the background of a

rotating GB black hole

$$\rho^2 \frac{dt}{d\lambda} = a(l - aE \sin^2 \theta) + \frac{r^2 + a^2}{\Delta} (E(r^2 + a^2) - al), \quad (44)$$

$$\rho^2 \frac{dr}{d\lambda} = \pm \sqrt{\mathcal{R}}, \quad (45)$$

$$\rho^2 \frac{d\theta}{d\lambda} = \pm \sqrt{\Theta}, \quad (46)$$

$$\rho^2 \frac{d\phi}{d\lambda} = (l \csc^2 \theta - aE) + \frac{a}{\Delta} (E(r^2 + a^2) - al). \quad (47)$$

Now we focus on the circular photon orbits by analyzing the radial motion. Since we consider the motion of photon, we take $\mu^2 = 0$ in the following. The radial motion (45) can be reexpressed as

$$\left(\rho^2 \frac{dr}{d\lambda} \right)^2 + V_{eff} = 0. \quad (48)$$

The effective potential reads

$$V_{eff}/E^2 = - \left[(r^2 + a^2) - a\xi \right]^2 + \Delta \left[\eta + (\xi - a)^2 \right], \quad (49)$$

where $\xi = l/E$ and $\eta = \mathcal{K}/E^2$, and the function Δ is given in Eq. (32). The unstable circular photon orbit satisfies the following conditions

$$V_{eff} = 0, \quad \frac{\partial V_{eff}}{\partial r} = 0, \quad \frac{\partial^2 V_{eff}}{\partial r^2} < 0. \quad (50)$$

The third condition ensures the orbit is unstable. Solving them, we obtain

$$\xi = \frac{(a^2 + r^2) \Delta' - 4\Delta r}{a\Delta'}, \quad (51)$$

$$\eta = \frac{r^2 (16\Delta (a^2 - \Delta) - r^2 \Delta'^2 + 8\Delta r \Delta')}{a^2 \Delta'^2}, \quad (52)$$

where the prime denotes the derivative with respect to r . Inserting them into the unstable condition (50), it requires that the radius of the unstable orbit satisfies

$$r + 2 \frac{\Delta}{\Delta'^2} (\Delta' - r\Delta'') > 0, \quad (53)$$

where we have used $\Delta > 0$ outside the horizon. It is easy to check that this condition holds for the Schwarzschild black hole, where $a = \alpha = 0$, and the radius $r = 3M$ of the photon sphere. This can also be numerically checked for the rotating GB black hole.

IV. BLACK HOLE SHADOWS AND OBSERVABLES

In this section, we would like to study the shadows cast by the nonrotating and rotating GB black holes. Before performing the study, it is worthwhile pointing out that in our case, all light sources are located at infinity and distributed uniformly in all directions. The observer is likewise located at infinity.

In order to describe the shadow under our assumption, one needs to introduce two celestial coordinates [12]

$$X = \lim_{r \rightarrow \infty} \left(-r^2 \sin \theta \frac{d\phi}{dr} \Big|_{\theta \rightarrow \theta_0} \right) = -\xi \csc \theta_0, \quad (54)$$

$$Y = \lim_{r \rightarrow \infty} \left(r^2 \frac{d\theta}{dr} \Big|_{\theta \rightarrow \theta_0} \right) = \pm \sqrt{\eta + a^2 \cos^2 \theta_0 - \xi^2 \cot^2 \theta_0}, \quad (55)$$

where the equations of motion (44)-(47) are used, and θ_0 is the inclination angle of the observer. If the observer locates on the equatorial plane, these celestial coordinates simplify to

$$X = -\xi \quad (56)$$

$$Y = \pm \sqrt{\eta}. \quad (57)$$

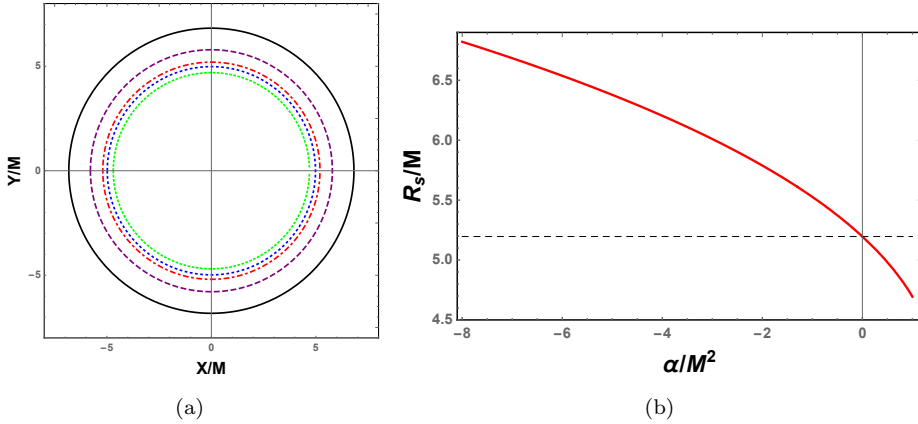


FIG. 2: (a) Shadows cast by the nonrotating GB black holes with $\alpha/M^2 = -8, -2, 0, 0.5$, and 1 from outside to inside. (b) The radius of the shadows as a function of α .

The shadow can be obtained by producing a parametric plot in the X - Y celestial plane consistent with Eqs. (51) and (52), where the parameter governing the plot is r . Such region is actually not illuminated by the photon sources. The boundary of the shadow can be determined by the radius of the circular photon orbits.

A. Nonrotating black hole shadows

Here we first consider the nonrotating black hole case, i.e., $a=0$, which is described by the metric (1). On the other hand, because the spherically symmetry of the black hole, the inclination angle of the observer effectively equals to $\theta_0 = \pi/2$.

For this nonrotating black hole with $a=0$, the unstable orbit is just the photon sphere of the black hole. Solving the first two conditions in (50), one can easily obtain the photon sphere radius r_{ps} , which is [75]

$$r_{\text{ps}} = 2\sqrt{3}M \cos\left(\frac{1}{3}\arccos\left(-\frac{4\alpha}{3\sqrt{3}M^2}\right)\right). \quad (58)$$

When $\alpha = 0$, this gives $r_{\text{ps}} = 3M$, which is just the result of the Schwarzschild black hole case. When α takes its upper and lower bounds, i.e., $-8M^2$ and M^2 , we have $r_{\text{ps}} = 4.7428M$ and $2.3723M$, respectively. The relation (58) shows that r_{ps} decreases with α . Moreover, it is easy to check the condition (53).

The black hole shadow is round in this case. Employing the photon sphere radius r_{ps} , we can find the radius of the black hole shadow. After a simple calculation, we obtain the equation describing the boundary of the black hole shadow, which is given by

$$X^2 + Y^2 = R_s^2, \quad (59)$$

where R_s denotes the radius of the shadow

$$R_s = \sqrt{\frac{2\alpha r_{\text{ps}}^2}{2\alpha - \sqrt{8\alpha r_{\text{ps}} + r_{\text{ps}}^4 + r_{\text{ps}}^2}}}. \quad (60)$$

In Fig. 2(a), we show the shadows for the nonrotating GB black holes with $\alpha/M^2 = -8, -2, 0, 0.5$, and 1 from outside to inside. Obviously, the shadow shrinks with the increase of α . The radius R_s of the shadow is also plotted as a function of α in Fig. 2(b). We can see that positive α shrinks the shadow and negative one enlarges the shadow.

In the following subsection, we will show that the influence of the black hole spin on the size of the shadow is very tiny, and the shadow size is mainly dependent on the GB coupling α .

B. Rotating black hole shadows

When the black hole spin is included, the shape of the shadow behaves quite differently. The critical photons moving from two different sides of the black hole have different values of ξ and η . This effect makes the black hole

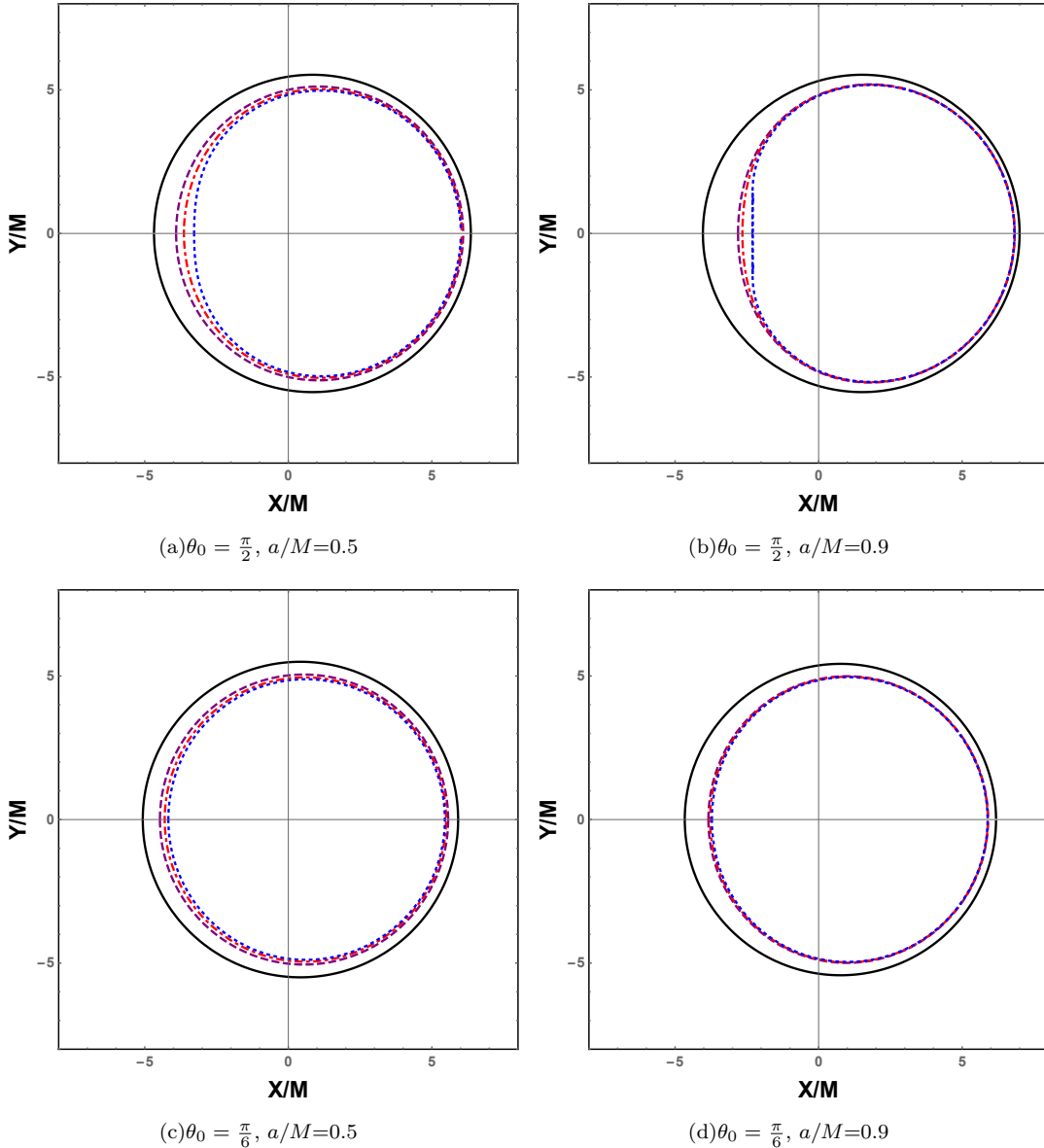


FIG. 3: Shadows of the rotating GB black holes. In the left panel, $\alpha/M^2=-1.0, 0.2, 0.4$, and 0.5157 from outside to inside. In the right panel, $\alpha/M^2=-1, 0.01, 0.04$, and 0.0648 from outside to inside.

shadow be elongated in the direction of the spin axis. So for a rotating black hole shadow, its shape is not a round but a distorted one. In this subsection, we focus on the shadow shapes cast by the rotating GB black holes.

Making use of (54) and (55), we plot the shadows for the rotating GB black holes in Fig. 3. All these figures show that the shadow shrinks with the increase of α . Moreover, when the black hole spin approaches its maximal value, the shadows get more deformed. However, when the inclination angle of the observer decreases such that $\theta_0 = \pi/6$, the shadows get less deformed when its spin approaches the maximal value. As a brief summary, we can conclude that the black hole shadow size is mainly dependent of α , while its distortion is dependent of the black hole spin a .

In order to get the black hole parameters through fitting the observed data, observables play a key role. The size and distortion are two important aspects of the shadows. So most of the observables are constructed through this fact. For clear, the schematic picture of the black hole shadow is given in Fig. 4 for nonvanishing spin. There are four characteristic points, the right point $(X_r, 0)$, left point $(X_l, 0)$, top point (X_t, Y_t) and bottom point (X_b, Y_b) of the shape. Considering the symmetry, one has $X_t = X_b$ and $Y_t = -Y_b$. As suggested in Ref. [14], the size of the shadow can be approximately measured by the radius R_s of the reference circle, which is just the circle passing the right, top, and bottom points of the shadow. Its center C is also on the X axis. The reference circle cuts the X axis

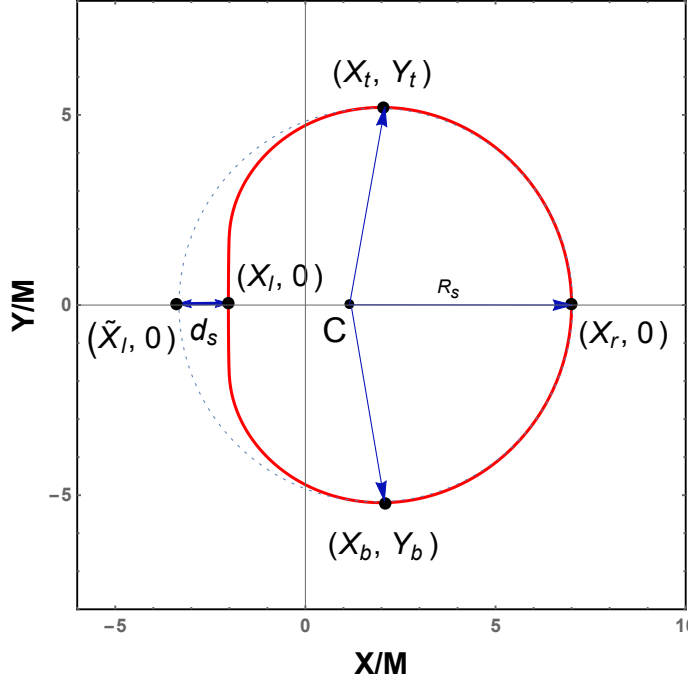


FIG. 4: Schematic picture of the black hole shadow with nonvanishing spin.

at $(\tilde{X}_l, 0)$. For a shadow cast by a nonrotating black hole, we will have $\tilde{X}_l = X_l$. However, the spin will departure these two points, and the shadow shape gets distorted. Another observable δ_s is also given in Ref. [14] to measure the distortion of the shadow with respect to the reference circle. In the following, we will study these observables as function of the GB coupling parameter α .

From the geometry of the shadow, the observables R_s and δ_s can be expressed with the coordinates of these characteristic points as

$$R_s = \frac{(X_t - X_r)^2 + Y_t^2}{2(X_r - X_t)}, \quad (61)$$

$$\delta_s = \frac{d_s}{R_s} = \frac{X_l - \tilde{X}_l}{R_s}. \quad (62)$$

Recently, the ratio k of two diameters ΔX and ΔY attracts much more attention. It is a new observable that can be fitted by the data of M87*. In terms of these coordinates, the ratio reads

$$k_s = \frac{\Delta Y}{\Delta X} = \frac{Y_t - Y_b}{X_r - X_l} = \frac{2Y_t}{(2 - \delta_s)R_s}. \quad (63)$$

where we have used the relations $\tilde{X}_l = X_r - 2R_s$. So it is clear that these observables are not independent of each other. As shown in Fig. 3, we can see that if a black hole spin is not very close to its maximum, the shadow is almost round. This conclusion is more true when the observer leaves the equatorial plane. Adopting this result, one has $R_s \approx 2Y_t$, and thus $k_s \approx 1/(2 - \delta_s)$. Moreover, since $\Delta Y \geq \Delta X$, we have $k_s \geq 1$.

For black hole spin $a/M=0.1, 0.3, 0.5$, and 0.9 , we calculate these observables when $\theta_0=\pi/2$ and $\pi/6$. The results indicate that the influence of the spin is mainly on the maximum value of α , while on the shadow size R_s is very tiny. So we will not show them here. The behaviors of observables δ_s and k_s are exhibited in Fig. 5. From the figures, we find that both δ_s and k_s increase with α and a , while decrease with θ_0 . Further comparing with the Kerr black hole case, positive α will increase δ_s and k_s , while negative ones decrease them. For example, when $a/M=0.9$, the Kerr black hole has $\delta_s=13.87\%$ and $k_s=1.07$ for $\theta_0 = \pi/2$. Meanwhile, the rotating GB black hole can achieve $\delta_s=23.61\%$ and $k_s=1.13$, respectively. One can expect, these values get larger for high black hole spin.

In summary, we obtain the following result: 1) the shadow size R_s is mainly dependent of the GB coupling parameter α . Positive α decreases the size, while negative one increases it. 2) When the black hole approaches its extremal case, the shadow will have larger values of δ_s and k_s . We believe these results will provide us the information on how to constraint the black hole spin a and the GB coupling parameter α .

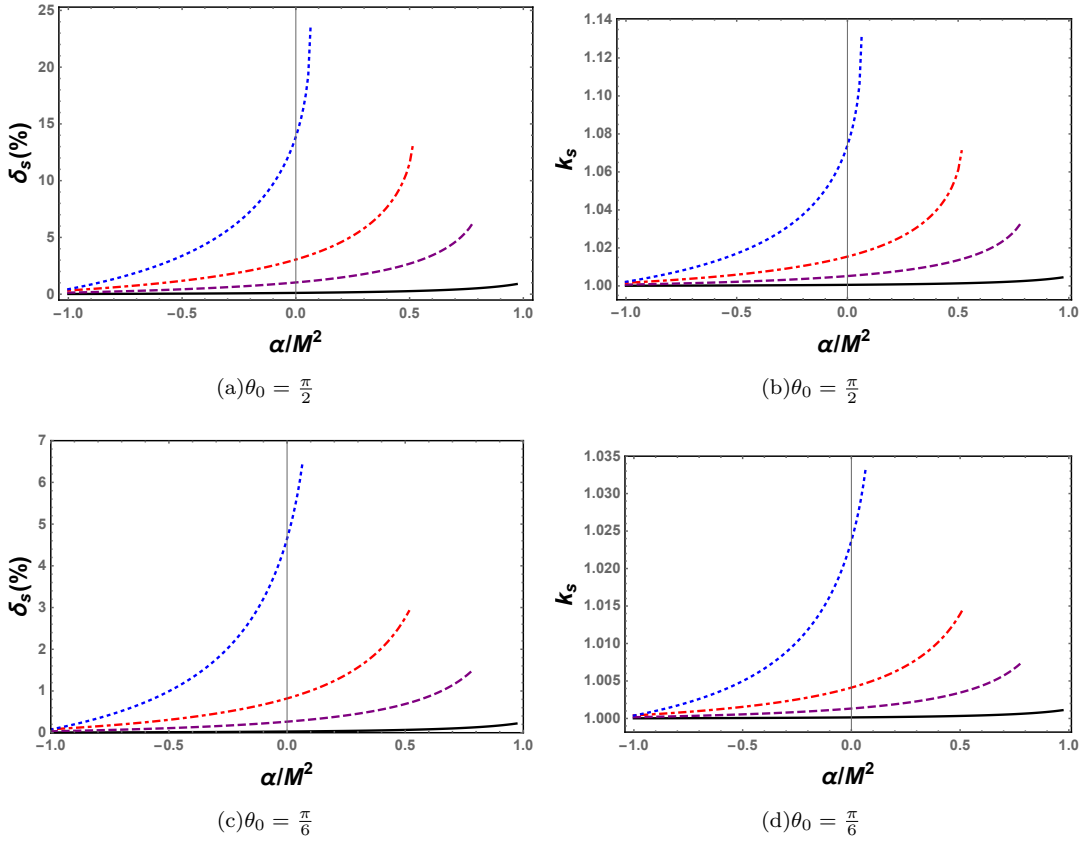


FIG. 5: Observables δ_s and k_s for the rotating GB black hole shadows. The spin is set as $a/M=0.1$ (black solid curve), 0.3 (dash purple curve), 0.5 (dotted dash red curve), and 0.9 (dotted blue curve) from bottom to top.

Before ending this section, we would like to note that here we only limit our attention in regions I and II, where the black hole always has one horizon at least. In region III, it denotes the naked singularity. Similarly, a naked singularity can also cast a shadow in the sky of an observer. However, its shadow is significantly different from the black hole shadow. Generally, the shadow shape of a naked singularity will not be a two-dimensional dark zone, while a one-dimensional opened dark arc. Considering that in a realistic scenario, the neighborhood of the arc will also be darkened, and thus there will be a dark lunate shape for the naked singularity. On the other side, if the value of the spin does not exceed the extreme case too much, the shape might similar to an extremal black hole. Surely, there is no evidence that the naked singularity can exist in our universe beyond the cosmic censorship conjecture. It is also worth to consider the shadow cast by a naked singularity. However, we only consider the black hole shadow in this paper, and the shadow of the naked singularity is a valuable issue for future.

V. SHADOW OF M87* AND GAUSS-BONNET COUPLING

In this section, we would like to use the result of the EHT Collaboration to fit the GB coupling by the observation of M87*.

For M87*, its observed shadow has an angular diameter of $42 \pm 3 \mu\text{as}$. The observation of the jet indicates that the inclination angle is about 17° [102]. Based on the stellar population measurements, the distance D of M87* from us was estimated to be $D=16.8 \pm 0.8 \text{ Mpc}$ [103–105]. The stellar dynamics and gas dynamics studies showed that the mass of M87* is about $6.2_{-0.5}^{+1.1} \times 10^9 M_\odot$ [106] and $3.5_{-0.3}^{+0.9} \times 10^9 M_\odot$ [107], respectively. Meanwhile, the EHT Collaboration reported that the mass of M87* is $6.5 \pm 0.7 \times 10^9 M_\odot$. Their result also implies that the absolute value of the dimensionless black hole spin a/M is in the range (0.5, 0.94).

For simplicity, we adopt the following data, $D=16.8 \text{ Mpc}$, $M=6.2 \times 10^9 M_\odot$, and $6.5 \times 10^9 M_\odot$. The inclination angle is chose to be 17° . According to the Blandford-Znajek mechanism, the jet of M87* is powered by the black hole spin. Thus we suppose that the inclination angle equals to the jet angle, and this result holds for this four-dimensional

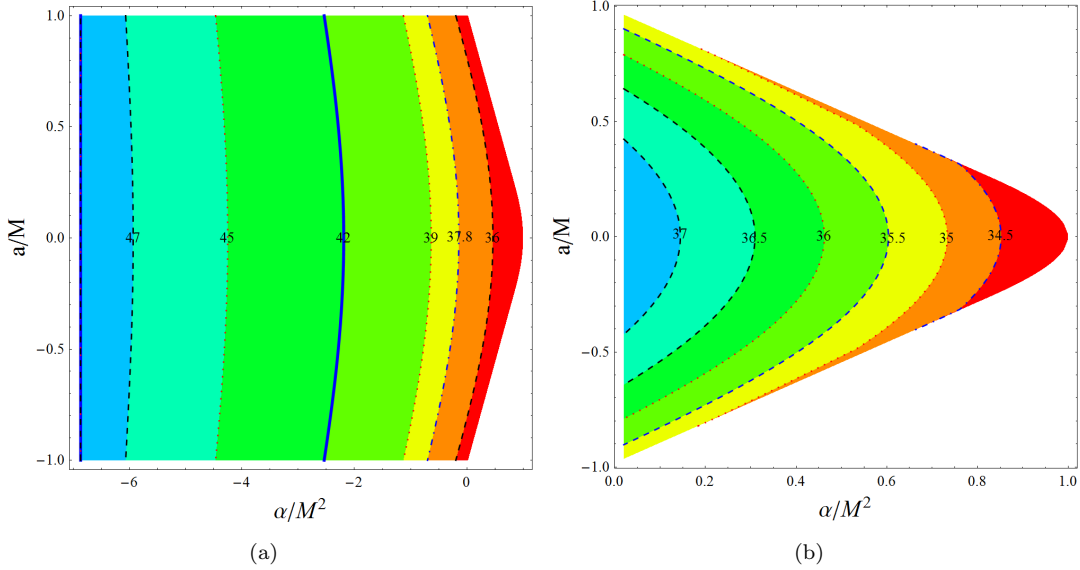


FIG. 6: Contours of the angular diameter of M87* in a/M - α/M^2 plane with $D=16.8$ Mpc, $M=6.2 \times 10^9 M_\odot$. (a) $\alpha/M^2 \in (-7, 1)$. (b) $\alpha/M^2 \in (0, 1)$.

GB black hole. Although as we show above, the rotating black hole solution only obeys the vacuum field equation on the equatorial plane. However, note that when matter fields are included, the field equation could be satisfied. So the choice of the inclination angle deviating from $\pi/2$ may be appropriate. Then we examine the average angular diameter $D_s = 2R_s$ with R_s given by (61) to fit the shadow size $42 \pm 3 \mu\text{as}$, or even 10% offset is considered.

First, we take $M=6.2 \times 10^9 M_\odot$ from the stellar dynamics, and show the contours of the angular diameter D_s of M87* in a/M - α/M^2 plane in Fig. 6. From Fig. 6(a), we see that α/M^2 is about in the range $(-4.5, -1)$ for the observed shadow diameter $42 \pm 3 \mu\text{as}$. Moreover even if the 10% offset of the diameter is taken into account, which reduces the corresponding angular diameter to $37.8 \mu\text{as}$, the associated GB coupling $\alpha/M^2 = -0.28$ and -0.62 for $|a/M| = 0.5$ and 0.9 , respectively. Therefore, the observation favors negative values of the GB coupling α . For clarity, we also show the contours in $\alpha/M^2 \in (0, 1)$ in Fig. 6(b). It is evident that in the positive range of α , the diameter is about in $34 \sim 37.5 \mu\text{as}$, which obviously lies out the observation.

When taking the mass of M87* $M=6.5 \times 10^9 M_\odot$ given by the EHT Collaboration, we plot the corresponding contours in Fig. 7. For $D_s \in (39, 45) \mu\text{as}$, it also falls in the range of negative α . While taking into account of the 10% offset of the diameter such that $D_s = 37.8 \mu\text{as}$, α/M^2 takes 0.26 for $a/M = 0.5$. However when $a/M > 0.83$, α will become negative, i.e., $\alpha/M^2 = -0.05$ for $a/M = 0.94$.

In summary, combining with the mass estimated from the stellar dynamics or by the EHT Collaboration, the observation favors $\alpha/M^2 \in (-4.5, 0)$ when considering the black hole spin $a/M \in (0.5, 0.94)$. Therefore, modeling M87* with a rotating GB black hole, astronomical observation favors a negative GB coupling constant.

VI. CONCLUSIONS AND DISCUSSIONS

In this paper, we first constructed a four-dimensional rotating GB black holes by using the NJ algorithm. Then, we studied the geodesics of a particle moving in this background. Employing the null geodesics, we investigated the shadow cast by nonrotating and rotating black holes. At last, by combining with the observation of M87*, we constrained the possible range of the GB coupling parameter.

For the nonrotating black hole in the case of positive GB coupling parameter α , the property of its horizon is similar to the charged black hole. Black hole with two horizons and naked singularity are bounded by the extremal black hole with $\alpha = M^2$. While for the negative α case, it was found that at the short radial distances, the spacetime has no real solution. However, if this range is hidden behind the horizon, the solution appears as a well behaved external solution. Thus, the study can be extended to $\alpha/M^2 = -8$.

For the rotating black hole case, the horizon will be deformed by the black hole spin. However, the major property is still unchanged. As shown above, we have $-8 \leq \alpha/M^2 \leq 1$ and $-2 \leq a/M \leq 2$. The particular details were given

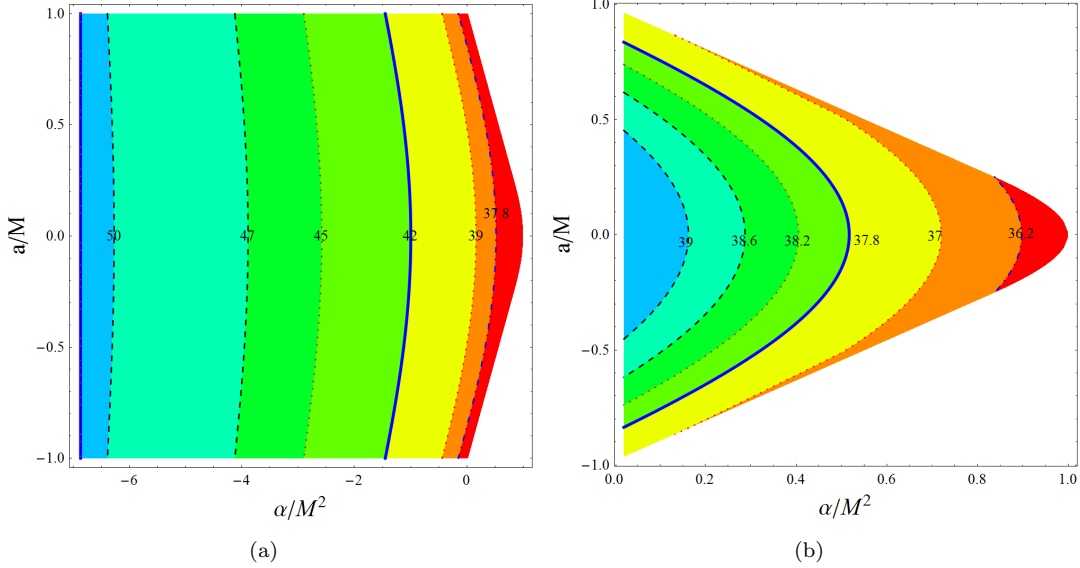


FIG. 7: Contours of the angular diameter of M87* in a/M - α/M^2 plane with $D=16.8$ Mpc, $M = 6.5 \times 10^9 M_\odot$. (a) $\alpha/M^2 \in (-7, 1)$. (b) $\alpha/M^2 \in (0, 1)$.

in Fig. 1.

The geodesics of a particle moving in the GB black hole background was solved following the Hamilton-Jacobi approach, which was also found to be a Kerr-like result. Based on the null geodesics, the shadow in the celestial coordinates was displayed. We observed that the shadow size is mainly dependent of α , for example, positive α decreases the size while negative one increases it. On the other hand, the distortion mainly depends on the black hole spin and the extremal bound. The distortion δ_s and the ratio k_s of these two diameters were also studied. Both them increase with a and α . Comparing with the Kerr black hole case, δ_s and k_s increase with positive α and decrease with the negative one. These results reveal the particular property of the GB coupling on the shadow shape.

Finally, we modeled M87* with this rotating GB black hole, and used the observation to constraint the possible range of the GB coupling parameter. Considering the inclination angle $\theta_0 = 17^\circ$ from the observation of the jet and the distance $D = 16.8$ Mpc from stellar population measurements, we plotted the contours of the angular diameter of the rotating GB black hole with $M = 6.2 \times 10^9 M_\odot$ and $6.5 \times 10^9 M_\odot$ from the stellar dynamics and EHT Collaboration, respectively. Comparing with the angular diameter $42 \pm 3 \mu\text{as}$ of M87*, our result supports that the GB parameter α is negative. Even if the 10% offset of the diameter is taken into account, the most possible range still falls in the negative α region.

Although the EHT Collaboration molded M87* with the Kerr black hole, and confirmed that the observation supports the GR, it also leaves us a possible window to test modified gravity due to the resolution of the observation and the unknown mass of the accretion of M87*. Combing with these two different mass data of M87*, our results favor that the GB coupling should fall in the possible negative range $\alpha/M^2 \in (-4.5, 0)$ or take very small positive values.

Since the four-dimensional GB black hole solution has just been discovered, it is worth to constraint the GB coupling parameter from other astronomical observations. This also provides us a promising way to understand GB gravity in four dimensions.

Note that the shadow was also studied in Ref. [101] after us for the same black hole solution. They calculated the area and oblateness of the shadow and then found that the rotating black hole is consistent with M87* within a finite parameter space. Here we investigated the distortion and oblateness of the shadow, and then fitted the angular diameter with M87* data. It is worth to mention that in our approach, we also considered the negative GB coupling parameter. Although there is no real solution at short distance, it is always hidden behind the outer horizon. Therefore, such parameter range is also worth to be examined.

Acknowledgements

We would like to thank Dr. M. Guo for useful discussions about the rotating black hole. This work was supported by the National Natural Science Foundation of China (Grants No. 11675064 and No. 11875151) and the Fundamental Research Funds for the Central Universities (Grants No. lzujbky-2019-ct06).

[1] K. Akiyama et al. [Event Horizon Telescope Collaboration], *First M87 Event Horizon Telescope Results. I. The Shadow of the Supermassive Black Hole*, *Astrophys. J.* **875**, L1 (2019), [arXiv:1906.11238 [astro-ph.GA]].

[2] K. Akiyama et al. [Event Horizon Telescope Collaboration], *First M87 Event Horizon Telescope Results. II. Array and Instrumentation*, *Astrophys. J.* **875**, L2 (2019), [arXiv:1906.11239 [astro-ph.IM]].

[3] K. Akiyama et al. [Event Horizon Telescope Collaboration], *First M87 Event Horizon Telescope Results. III. Data Processing and Calibration*, *Astrophys. J.* **875**, L3 (2019), [arXiv:1906.11240 [astro-ph.GA]].

[4] K. Akiyama et al. [Event Horizon Telescope Collaboration], *First M87 Event Horizon Telescope Results. IV. Imaging the Central Supermassive Black Hole*, *Astrophys. J.* **875**, L4 (2019), [arXiv:1906.11241 [astro-ph.GA]].

[5] K. Akiyama et al. [Event Horizon Telescope Collaboration], *First M87 Event Horizon Telescope Results. V. Physical Origin of the Asymmetric Ring*, *Astrophys. J.* **875**, L5 (2019), [arXiv:1906.11242 [astro-ph.GA]].

[6] K. Akiyama et al. [Event Horizon Telescope Collaboration], *First M87 Event Horizon Telescope Results. VI. The Shadow and Mass of the Central Black Hole*, *Astrophys. J.* **875**, L6 (2019), [arXiv:1906.11243 [astro-ph.GA]].

[7] A. M. Hughes, A. Beasley, and C. Carilli, *Next Generation Very Large Array: Centimeter Radio Astronomy in the 2020s*, *IAU General Assembly* **22**, 2255106 (2015).

[8] G. H. Sanders, *The Thirty Meter Telescope (TMT): An International Observatory*, *Journal of Astrophysics and Astronomy* **34**, 81 (2013).

[9] C. Goddi et al., *BlackHoleCam: Fundamental physics of the galactic center*, *Int. J. Mod. Phys. D* **26**, 1730001 (2016), [arXiv:1606.08879 [astro-ph.HE]].

[10] J. L. Synge, *The escape of photons from gravitationally intense stars*, *Mon. Not. Roy. Astron. Soc.*, **131**, 463 (1966).

[11] J. P. Luminet, *Image of a spherical black hole with thin accretion disk*, *Journal of Astrophysics and Astronomy*, **75**, 228 (1979).

[12] J. M. Bardeen, *Timelike and null geodesics in the Kerr metric*, in *Proceedings of the Ecole de Physique Thorique: Les Astres Occlus: Les Houches, France, 1972*, edited by C. Dewitt and B. S. Dewitt (Gordon & Breach Science Publishers, France, 1973).

[13] S. Chandrasekhar, *The Mathematical Theory of Black Holes*, Oxford University Press, New York, (1992).

[14] K. Hioki and K. I. Maeda, *Measurement of the Kerr Spin Parameter by Observation of a Compact Object's Shadow*, *Phys. Rev. D* **80**, 024042 (2009), [arXiv:0904.3575 [astro-ph.HE]].

[15] L. Amarilla and E. F. Eiroa, *Shadow of a rotating braneworld black hole*, *Phys. Rev. D* **85**, 064019 (2012), [arXiv:1112.6349 [gr-qc]].

[16] T. Johannsen, *Photon rings around Kerr and Kerr-like black holes*, *Astrophys. J.* **777**, 170 (2013), [arXiv:1501.02814 [astro-ph.HE]].

[17] M. Ghasemi-Nodehi, Z.-L. Li, and C. Bambi, *Shadows of CPR black holes and tests of the Kerr metric*, *Eur. Phys. J. C* **75**, 315 (2015), [arXiv:1506.02627 [gr-qc]].

[18] C. Bambi and K. Freese, *Apparent shape of super-spinning black holes*, *Phys. Rev. D* **79**, 043002 (2009), [arXiv:0812.1328 [astro-ph]];

[19] L. Amarilla, E. F. Eiroa, and G. Giribet, *Null geodesics and shadow of a rotating black hole in extended Chern-Simons modified gravity*, *Phys. Rev. D* **81**, 124045 (2010), [arXiv:1005.0607 [gr-qc]].

[20] Z. Stuchlik and J. Schee, *Appearance of Keplerian discs orbiting Kerr superspinars*, *Class. Quant. Grav.* **27**, 215017 (2010), [arXiv:1101.3569 [gr-qc]].

[21] L. Amarilla and E. F. Eiroa, *Shadow of a Kaluza-Klein rotating dilaton black hole*, *Phys. Rev. D* **87**, 044057 (2013), [arXiv:1301.0532 [gr-qc]].

[22] P. G. Nedkova, V. K. Tinchev, and S. S. Yazadjiev, *The shadow of a rotating traversable wormhole*, Phys. Rev. D **88**, 124019, (2013) [arXiv:1307.7647 [gr-qc]].

[23] S.-W. Wei and Y.-X. Liu, *Observing the shadow of Einstein-Maxwell-Dilaton-Axion black hole*, JCAP **1311**, 063 (2013), [arXiv:1311.4251 [gr-qc]].

[24] N. Tsukamoto, Z.-L. Li, and C. Bambi, *Constraining the spin and the deformation parameters from the black hole shadow*, JCAP **1406**, 043 (2014), [arXiv:1403.0371 [gr-qc]].

[25] C. Bambi and N. Yoshida, *Shape and position of the shadow in the $\delta=2$ Tomimatsu-Sato space-time*, Class. Quant. Grav. **27**, 205006 (2010), [arXiv:1004.3149 [gr-qc]].

[26] F. Atamurotov, A. Abdujabbarov, and B. Ahmedov, *Shadow of rotating non-Kerr black hole*, Phys. Rev. D **88**, 064004 (2013).

[27] S. Abdolrahimi, R. B. Mann, and C. Tzounis, *Distorted local shadows*, Phys. Rev. D **91**, 084052 (2015), [arXiv:1502.00073 [gr-qc]].

[28] S.-W. Wei, P. Cheng, Y. Zhong, and X.-N. Zhou, *Shadow of noncommutative geometry inspired black hole*, JCAP **1508**, 004 (2015), [arXiv:1501.06298 [gr-qc]].

[29] F. Atamurotov, B. Ahmedov, and A. Abdujabbarov, *Optical properties of black hole in the presence of plasma: shadow*, Phys. Rev. D **92**, 084005 (2015), [arXiv:1507.08131 [gr-qc]].

[30] A. Abdujabbarov, M. Amir, B. Ahmedov, and S. G. Ghosh, *Shadow of rotating regular black holes*, Phys. Rev. D **93**, 104004 (2016), [arXiv:1604.03809 [gr-qc]].

[31] M.-Z. Wang, S.-B. Chen, and J.-L. Jing, *Shadow casted by a Konoplya-Zhidenko rotating non-Kerr black hole*, JCAP **1710**, 051 (2017), [arXiv:1707.09451 [gr-qc]].

[32] M. Amir, B. P. Singh, and S. G. Ghosh, *Shadows of rotating five-dimensional charged EMCS black holes*, Eur. Phys. J. C **78**, 399 (2018), [arXiv:1707.09521 [gr-qc]].

[33] N. Tsukamoto, *Black hole shadow in an asymptotically-flat, stationary, and axisymmetric spacetime: The Kerr-Newman and rotating regular black holes*, Phys. Rev. D **97**, 064021 (2018), [arXiv:1708.07427 [gr-qc]].

[34] M.-Z. Wang, S.-B. Chen, and J.-L. Jing, *Shadows of Bonnor black dihole by chaotic lensing*, Phys. Rev. D **97**, 064029 (2018), [arXiv:1710.07172 [gr-qc]].

[35] R. Shaikh, *Shadows of rotating wormholes*, Phys. Rev. D **98**, 024044 (2018), [arXiv:1803.11422 [gr-qc]].

[36] X. Hou, Z.-Y. Xu, M. Zhou, and J.-C. Wang, *Black hole shadow of Sgr A* in dark matter halo*, JCAP **1807**, 015 (2018), [arXiv:1804.08110 [gr-qc]].

[37] P. V. P. Cunha, C. A. R. Herdeiro, E. Radu, and H. F. Runarsson, *Shadows of Kerr black holes with scalar hair*, Phys. Rev. Lett. **115**, 211102 (2015), [arXiv:1509.00021 [gr-qc]].

[38] P. V. P. Cunha, C. A. R. Herdeiro, and E. Radu, *Fundamental photon orbits: black hole shadows and spacetime instabilities*, Phys. Rev. D **96**, 024039 (2017), [arXiv:1705.05461 [gr-qc]].

[39] P. V. P. Cunha and C. A. R. Herdeiro, *Shadows and strong gravitational lensing: a brief review*, Gen. Rel. Grav. **50**, 42 (2018), [arXiv:1801.00860 [gr-qc]].

[40] O. Yu. Tsupko, *Analytical calculation of black hole spin using deformation of the shadow*, Phys. Rev. D **95**, 104058 (2017), [arXiv:1702.04005 [gr-qc]].

[41] V. Perlick, O. Yu. Tsupko, and G. S. Bisnovatyi-Kogan, *Black hole shadow in an expanding universe with a cosmological constant*, Phys. Rev. D **97**, 104062 (2018), [arXiv:1804.04898 [gr-qc]].

[42] R. Shaikh, P. Kocherlakota, R. Narayan, and P. S. Joshi, *Shadows of spherically symmetric black holes and naked singularities*, Mon. Not. Roy. Astron. Soc. **482**, 52 (2019), [arXiv:1802.08060 [astro-ph.HE]].

[43] H.-M. Wang, Y.-M. Xu, and S.-W. Wei, *Shadows of Kerr-like black holes in a modified gravity theory*, JCAP **1903**, 046 (2019), [arXiv:1810.12767 [gr-qc]].

[44] S.-W. Wei, Y.-X. Liu, and R. B. Mann, *Intrinsic curvature and topology of shadow in Kerr spacetime*, Phys. Rev. D **99**, 041303(R) (2019), [arXiv:1811.00047 [gr-qc]].

[45] S.-W. Wei, Y.-C. Zou, Y.-X. Liu, and R. B. Mann, *Curvature radius and Kerr black hole shadow*, JCAP **1908**, 030 (2019), [arXiv:1904.07710 [gr-qc]].

[46] Z. Younsi, A. Zhidenko, L. Rezzolla, R. Konoplya, and Y. Mizuno, *New method for shadow calculations: Application to parametrized axisymmetric black holes*, Phys. Rev. D **94**, 084025 (2016) [arXiv:1607.05767 [gr-qc]].

[47] A. K. Mishra, S. Chakraborty, and S. Sarkar, *Understanding photon sphere and black hole shadow in dynamically evolving spacetimes*, Phys. Rev. D **99**, 104080 (2019), [arXiv:1903.06376 [gr-qc]].

[48] A. B. Abdikamalov, A. A. Abdujabbarov, D. Malafarina, C. Bambi, and B. Ahmedov, *A black hole mimicker hiding in the shadow: Optical properties of the γ metric*, Phys. Rev. D **100**, 024014 (2019), [arXiv:1904.06207 [gr-qc]].

[49] A. A. Abdujabbarov, L. Rezzolla, and B. J. Ahmedov, *A coordinate-independent characterization of a black hole shadow*, Mon. Not. Roy. Astron. Soc. **454**, 2423 (2015), [arXiv:1503.09054 [gr-qc]].

[50] R. Shaikh, *Black hole shadow in a general rotating spacetime obtained through Newman-Janis algorithm*, Phys. Rev. D **100**, 024028 (2019), [arXiv:1904.08322 [gr-qc]].

[51] M. Wang, S. Chen, J. Wang, and J. Jing, *Shadow of a Schwarzschild black hole surrounded by a Bach-Weyl ring*, Eur. Phys. J. C **80**, 110 (2020), [arXiv:1904.12423 [gr-qc]].

[52] C. Bambi, K. Freese, S. Vagnozzi, and L. Visinelli, *Testing the rotational nature of the supermassive object M87* from the circularity and size of its first image*, Phys. Rev. D **100**, 044057 (2019), [arXiv:1904.12983 [gr-qc]].

[53] R. A. Konoplya, *Shadow of a black hole surrounded by dark matter*, Phys. Lett. B **795**, 1 (2019), [arXiv:1905.00064 [gr-qc]].

[54] S. Vagnozzi and L. Visinelli, *Hunting for extra dimensions in the shadow of M87**, Phys. Rev. D **100**, 024020 (2019), [arXiv:1905.12421 [gr-qc]].

[55] T. Zhu, Q. Wu, M. Jamil, and K. Jusufi, *Shadows and deflection angle of charged and slowly rotating black holes in Einstein-aether theory*, Phys. Rev. D **100**, 044055 (2019), [arXiv:1906.05673 [gr-qc]].

[56] I. Banerjee, S. Chakraborty, and S. SenGupta, *Silhouette of M87*: A new window to peek into the world of hidden dimensions*, Phys. Rev. D **101**, 041301 (2020), [arXiv:1909.09385 [gr-qc]].

[57] H. Lu, H.-D. Lyu, *On the Size of a Black Hole: The Schwarzschild is the Biggest*, Phys. Rev. D **101**, 044059 (2020), [arXiv:1911.02019 [gr-qc]].

[58] X.-H. Feng and H. Lu, *On the Size of Rotating Black Holes*, Eur. Phys. J. C **80**, 551 (2020), [arXiv:1911.12368 [gr-qc]].

[59] C. Li, S.-F. Yan, L. Xue, X. Ren, Y.-F. Cai, D. A. Easson, Y.-F. Yuan, and H. Zhao, *Testing the equivalence principle via the shadow of black holes*, Phys. Rev. Res. **2**, 023164 (2020), [arXiv:1912.12629 [astro-ph.CO]].

[60] P.-C. Li, M. Guo, and B. Chen, *Shadow of a Spinning Black Hole in an Expanding Universe*, Phys. Rev. D **101**, 084041 (2020), [arXiv:2001.04231 [gr-qc]].

[61] C. Liu, T. Zhu, Q. Wu, K. Jusufi, M. Jamil, M. Azreg-Ainou, and A. Wang, *Shadow and Quasinormal Modes of a Rotating Loop Quantum Black Hole*, Phys. Rev. D **101**, 084001 (2020), [arXiv:2003.00477 [gr-qc]].

[62] J. W. Moffat and V. T. Toth, *The masses and shadows of the black holes Sagittarius A* and M87* in modified gravity (MOG)*, Phys. Rev. D **101**, 024014 (2020), [arXiv:1904.04142 [gr-qc]].

[63] H. Davoudiasl and P. B. Denton, *Ultra Light Boson Dark Matter and Event Horizon Telescope Observations of M87**, Phys. Rev. Lett. **123**, 021102 (2019), [arXiv:1904.09242 [astro-ph.CO]].

[64] N. Bar, K. Blum, T. Lacroix, and P. Panci, *Looking for ultralight dark matter near supermassive black holes*, JCAP **07**, 045 (2019), [arXiv:1905.11745 [astro-ph.CO]].

[65] S. X. Tian and Z.-H. Zhu, *Testing the Schwarzschild metric in a strong field region with the Event Horizon Telescope*, Phys. Rev. D **100**, 064011 (2019), [arXiv:1908.11794 [gr-qc]].

[66] R. Kumar, S. G. Ghosh, and A. Wang, *Shadow cast and deflection of light by charged rotating regular black holes*, Phys. Rev. D **100**, 124024 (2019), [arXiv:1912.05154 [gr-qc]].

[67] A. Allahyari, M. Khodadi, S. Vagnozzi, and D. F. Mota, *Magnetically charged black holes from non-linear electrodynamics and the Event Horizon Telescope*, JCAP **2002**, 003 (2020), [arXiv:1912.08231 [gr-qc]].

[68] M. Rummel and C.P. Burgess, *Constraining Fundamental Physics with the Event Horizon Telescope*, JCAP **05**, 051 (2020), [arXiv:2001.00041 [gr-qc]].

[69] R. Kumar, S. G. Ghosh, and A. Wang, *Light deflection and shadow cast by rotating Kalb-Ramond black holes*, Phys. Rev. D **101**, 104001 (2020), [arXiv:2001.00460 [gr-qc]].

[70] A. Narang, S. Mohanty, and A. Kumar, *Test of Kerr-Sen metric with black hole observations*, [arXiv:2002.12786 [gr-qc]].

[71] Y. Tomozawa, *Quantum corrections to gravity*, [arXiv:1107.1424 [gr-qc]].

[72] G. Cognola, R. Myrzakulov, L. Sebastiani, and S. Zerbini, *Einstein gravity with Gauss-Bonnet entropic corrections*, Phys. Rev. D, **88**, 024006 (2013), [arXiv:1304.1878 [gr-qc]].

[73] D. Glavan and C. Lin, *Einstein-Gauss-Bonnet Gravity in Four-Dimensional Spacetime*, Phys. Rev. Lett. **124**, 081301 (2020), [arXiv:1905.03601 [gr-qc]].

[74] R. A. Konoplya and A. F. Zinhailo, *Quasinormal modes, stability and shadows of a black hole in the novel 4D Einstein-Gauss-Bonnet gravity*, [arXiv:2003.01188 [gr-qc]].

[75] M. Guo and P.-C. Li, *The innermost stable circular orbit and shadow in the novel 4D Einstein-Gauss-Bonnet gravity*, Eur. Phys. J. C **80**, 588 (2020), [arXiv:2003.02523 [gr-qc]].

[76] P. G. S. Fernandes, *Charged Black Holes in AdS Spaces in 4D Einstein Gauss-Bonnet Gravity*, Phys. Lett. B **805**, 135468 (2020), [arXiv:2003.05491 [gr-qc]].

[77] A. Casalino, A. Colleaux, M. Rinaldi, and S. Vicentini, *Regularized Lovelock gravity*, [arXiv:2003.07068 [gr-qc]].

[78] H. Lu and Y. Pang, *Horndeski Gravity as $D \rightarrow 4$ Limit of Gauss-Bonnet*, [arXiv:2003.11552 [gr-qc]].

[79] W.-Y. Ai, *A note on the novel 4D Einstein-Gauss-Bonnet gravity*, Commun. Theor. Phys. **72**, 095402 (2020), [arXiv:2004.02858 [gr-qc]].

[80] M. Gurses, T. C. Sisman, and B. Tekin, *Is there a novel Einstein-Gauss-Bonnet theory in four dimensions?* Eur. Phys. J. C **80**, 647 (2020), [arXiv:2004.03390 [gr-qc]].

[81] S. Mahapatra, *A note on the total action of 4D Gauss-Bonnet theory*, [arXiv:2004.09214 [gr-qc]].

[82] R. A. Hennigar, D. Kubiznak, R. B. Mann, and C. Pollack, *Lower-dimensional Gauss-Bonnet Gravity and BTZ Black Holes*, Phys. Lett. B **808**, 135657 (2020), [arXiv:2004.12995 [gr-qc]].

[83] S. X. Tian and Z.-H. Zhu, *Comment on "Einstein-Gauss-Bonnet Gravity in Four-Dimensional Spacetime"*, [arXiv:2004.09954 [gr-qc]].

[84] J. Arrechea, A. Delhom, and A. Jimenez-Cano, *Yet another comment on four-dimensional Einstein-Gauss-Bonnet gravity*, [arXiv:2004.12998 [gr-qc]].

[85] K. Aoki, M. A. Gorji, and S. Mukohyama, *A consistent theory of $D \rightarrow 4$ Einstein-Gauss-Bonnet gravity*, arXiv:2005.03859 [gr-qc].

[86] Z.-C. Lin, K. Yang, S.-W. Wei, Y.-Q. Wang, and Y.-X. Liu, *Is the four-dimensional novel EGB theory equivalent to its regularized counterpart in a cylindrically symmetric spacetime?* arXiv:2006.07913 [gr-qc].

[87] H. Lu and Y. Pang, *Horndeski Gravity as $D \rightarrow 4$ Limit of Gauss-Bonnet*, arXiv:2003.11552 [gr-qc].

[88] P.G.S. Fernandes, P. Carrilho, T. Clifton, and D.J. Mulryne, *Derivation of Regularized Field Equations for the Einstein-Gauss-Bonnet Theory in Four Dimensions*, Phys. Rev. D **102**, 024025 (2020), arXiv:2004.08362 [gr-qc].

[89] R.A. Hennigar, D. Kubiznak, R.B. Mann, and C. Pollack, *On Taking the $D \rightarrow 4$ limit of Gauss-Bonnet Gravity: Theory and Solutions*, JHEP **07**, 027 (2020), [arXiv:2004.09472 [gr-qc]].

[90] E. T. Newman and A. I. Janis, *Note on the Kerr spinning particle metric*, J. Math. Phys. **6**, 915 (1965).

[91] D. Hansen and N. Yunes, *Applicability of the Newman-Janis Algorithm to Black Hole Solutions of Modified Gravity Theories*, Phys. Rev. D **88**, 104020 (2013), [arXiv:1308.6631 [gr-qc]].

[92] M. Azreg-Aïnou, *Generating rotating regular black hole solutions without complexification*, Phys. Rev. D **90**, 064041 (2014), [arXiv:1405.2569 [gr-qc]].

[93] P. V. P. Cunha, C. A. R. Herdeiro, B. Kleihaus, J. Kunz, and E. Radu, *Shadows of Einstein-dilaton-Gauss-Bonnet black holes*, Phys. Lett. B **768**, 373 (2017), [arXiv:1701.00079 [gr-qc]].

[94] D. G. Boulware and S. Deser, *String-Generated Gravity Models* Phys. Rev. Lett. **55**, 2656 (1985).

[95] D. L. Wiltshire, *Spherically symmetric solutions of Einstein-Maxwell theory with a Gauss-Bonnet term*, Phys. Lett. B **38**, 2445 (1988).

[96] R. G. Cai, *Gauss-Bonnet black holes in AdS spaces* Phys. Rev. D **65**, 084014 (2002), [arXiv:hep-th/0109133].

[97] S. Nojiri and S. D. Odintsov, *Anti-de Sitter Black Hole Thermodynamics in Higher Derivative Gravity and New Confining-Deconfining Phases in dual CFT*, Phys. Lett. B **521**, 87 (2001), [arXiv:hep-th/0109122].

[98] M. Cvetic, S. Nojiri, and S. D. Odintsov, *Black Hole Thermodynamics and Negative Entropy in deSitter and Anti-deSitter Einstein-Gauss-Bonnet gravity*, Nucl. Phys. B **628**, 295 (2002), [arXiv:hep-th/0112045].

[99] R.-G. Cai, L.-M. Cao, and N. Ohta, *Black Holes in Gravity with Conformal Anomaly and Logarithmic Term in Black Hole Entropy* JHEP **1004**, 082 (2010), [arXiv:0911.4379 [hep-th]].

[100] R.-G. Cai, *Thermodynamics of Conformal Anomaly Corrected Black Holes in AdS Space* Phys. Lett. B **733**, 183 (2014), [arXiv:1405.1246 [hep-th]].

- [101] R. Kumar and S. G. Ghosh, *Rotating black holes in the novel 4D Einstein-Gauss-Bonnet gravity*, JCAP **07**, 053 (2020), [arXiv:2003.08927 [gr-qc]].
- [102] R. C. Walker, P. E. Hardee, F. B. Davies, C. Ly, and W. Junor, *The Structure and Dynamics of the Sub-parsec Scale Jet in M87 Based on 50 VLBA Observations Over 17 Years at 43 GHz*, Astrophys. J. **855**, 128 (2018), [arXiv:1802.06166 [astro-ph.HE]].
- [103] J. P. Blakeslee, A. Jordan, S. Mei, P. Cote, L. Ferrarese, L. Infante, E. W. Peng, J. L. Tonry, and M. J. West, *The ACS for the Fornax cluster survey. V. Measurement and recalibration of surface brightness fluctuations and a precise value of the Fornax CVirgo relative distance*, Astrophys. J. **694**, 556 (2009), [arXiv:0901.1138 [astro-ph.CO]].
- [104] S. Bird, W. E. Harris, J. P. Blakeslee, and C. Flynn, *The inner halo of M87: A first direct view of the red-giant population*, Astron. Astrophys. **524**, A71 (2010), [arXiv:1009.3202 [astro-ph.GA]].
- [105] M. Cantiello et al., *A precise distance to the host galaxy of the binary neutron star merger GW170817 using surface brightness fluctuations*, Astrophys. J. **854**, L31 (2018), [arXiv:1801.06080 [astro-ph.GA]].
- [106] K. Gebhardt, J. Adams, D. Richstone, T.R. Lauer, S.M. Faber, K. Gultekin, J. Murphy, and S. Tremaine, *The black-hole mass in M87 from Gemini/NIFS adaptive optics observations*, Astrophys. J. **729**, 119 (2011), [arXiv:1101.1954 [astro-ph.CO]].
- [107] J. L. Walsh, A. J. Barth, L. C. Ho, and M. Sarzi, *The M87 black hole mass from gas-dynamical models of space telescope imaging spectrograph observations*, Astrophys. J. **770**, 86 (2013), [arXiv:1304.7273 [astro-ph.CO]].